

# Phase transition of the Ag/Si(111)-( $\sqrt{3} \times \sqrt{3}$ ) surface studied by photoelectron diffraction

Kazuyuki Sakamoto,<sup>1,\*</sup> Toshihiro Suzuki,<sup>2</sup> Kenji Mawatari,<sup>2</sup> Keisuke Kobayashi,<sup>2</sup> Jun Okabayashi,<sup>3</sup> Kanta Ono,<sup>4</sup> Nobuo Ueno,<sup>1</sup> and Masaharu Oshima<sup>3</sup>

<sup>1</sup>Graduate School of Science and Technology, Chiba University, Chiba 263-8522, Japan

<sup>2</sup>Department of Physics, Graduate School of Science, Tohoku University, Sendai, 980-8578, Japan

<sup>3</sup>Department of Applied Chemistry, The University of Tokyo, Tokyo 113-8656, Japan

<sup>4</sup>Institute of Materials Structure Science, High Energy Accelerator Research Organization, Tsukuba 305-0801, Japan

(Received 22 February 2006; published 5 May 2006)

The local atomic structure of the Ag induced Si(111)-( $\sqrt{3} \times \sqrt{3}$ ) surface has been investigated using photoelectron diffraction (PED) at 10 and 300 K. Two surface components, whose intensities varied by changing the photon energy as a consequence of diffraction effects, were observed in the Si 2*p* core-level spectra at both temperatures. The good agreement between the experimental PED patterns of the Si 2*p* surface components and the simulated PED patterns indicates that the atomic structure of this surface follows the inequivalent triangle model. Further, since the PED patterns obtained at 10 and 300 K resemble each other closely, we conclude that the local atomic structure of the Ag/Si(111)-( $\sqrt{3} \times \sqrt{3}$ ) surface is the same at the two temperatures, and thus that the origin of the transition reported in the literature is an order-disorder transition.

DOI: 10.1103/PhysRevB.73.193303

PACS number(s): 68.35.Rh, 68.43.Fg, 61.14.Qp, 79.60.-i

Semiconductor surfaces modified by adsorption of metal atoms have attracted much attention due to the possibility of observing various exotic low-dimensional physical phenomena.<sup>1,2</sup> Of the great number of monovalent atom-induced reconstructed semiconductor surfaces, the Si(111)-( $\sqrt{3} \times \sqrt{3}$ ) surface formed by the adsorption of one monolayer (ML) of Ag is one of the most well known. Extensive experimental and theoretical studies have been performed on the Ag/Si(111)-( $\sqrt{3} \times \sqrt{3}$ ) surface, and two types of transition have been reported to exist on this surface so far. One is a metal-semiconductor transition that is induced by the presence of additional monovalent atoms on the surface,<sup>3-6</sup> and the other one is a transition in the atomic structure of the surface. However, although the existence of the second transition is obvious from the fact that the scanning tunneling microscopy (STM) image observed at 62 K is different from the image observed at 300 K, the mechanism of this transition is not as well understood as that of the first transition.

The honeycomb-chain-trimer (HCT) model<sup>7-10</sup> agrees with the scanning tunneling microscopy (STM) image observed at 300 K, and thus the atomic structure of the Ag/Si(111)-( $\sqrt{3} \times \sqrt{3}$ ) surface has been widely accepted to be described by this model until the late 1990s. As shown in Fig. 1, the HCT model, which is characterized by Ag trimers that are arranged in a honeycomb lattice, belongs to the *p31m* space group with a mirror symmetry plane along the  $[11\bar{2}]$  axis (the two Ag trimers in the unit cell are equivalent). However, STM images that cannot be explained in accordance with this HCT model have been observed at 62 K in 1999,<sup>11,12</sup> and a new structural model has been proposed to explain these low-temperature STM images.<sup>11</sup> In this new model, which is called the inequivalent triangle (IET) model (*p3* space group), the Ag triangles (thin dashed line triangles) and the outermost Si trimers (first-layer Si atoms indicated by thin solid line triangles) are rotated  $6^\circ$  around the corner of the unit cell. As a consequence, the two Ag trimers in the unit cell become inequivalent and the mirror symmetry plane along the  $[11\bar{2}]$  axis disappears. Since there are two rota-

tional directions, the IET structure is classified into two domains, the IET(+) domain ( $\theta_{\text{Ag}}=66^\circ$ ,  $\theta_{\text{Si}}=54^\circ$ ) and the IET(-) domain ( $\theta_{\text{Ag}}=54^\circ$ ,  $\theta_{\text{Si}}=66^\circ$ ).

Based on first-principles calculation,<sup>11</sup> the IET model was reported to be energetically more stable than the HCT model. This proposition has been confirmed experimentally by using different techniques,<sup>11-17</sup> i.e., all the experimental studies performed after 1999 report that the atomic structure follows the IET model at low-temperature. However, in contrast to this common opinion for the low-temperature phase, the atomic structure of the room-temperature phase is still controversial. Even using the same experimental method, contradicting results have been reported. The determination of the atomic structure of the room-temperature phase is essential in order to understand the origin of the transition, i.e., whether a change in the surface structure from IET to HCT or a thermal fluctuation between the IET(+) and IET(-)

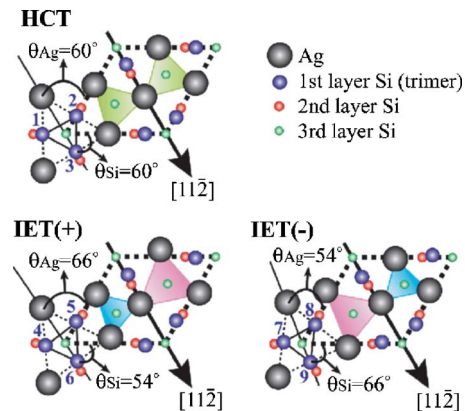


FIG. 1. (Color online) Schematic illustrations of the HCT, IET(+), and IET(-) models proposed for the Ag/Si(111)-( $\sqrt{3} \times \sqrt{3}$ ) surface. The thick dashed lines indicate the unit cell of each model and the shaded areas represent the Ag trimers. The difference between the three models is the angles  $\theta_{\text{Ag}}$  and  $\theta_{\text{Si}}$ , and the size of the areas of the Ag trimers.

structures that leads to a observation of the time-averaged structure in STM at room temperature. Since the former inconsistent reports mainly result from the fact that the method used in these studies is either a slow process or shows the average structure of a certain area, a method whose process is faster than the thermal fluctuation and gives information about the local structure is required. Photoelectron diffraction (PED) is a method that satisfies these two requirements.

In this paper, we present a PED study of the Ag-induced Si(111)-( $\sqrt{3} \times \sqrt{3}$ ) surface performed at 10 and 300 K. Two surface components were observed in the Si 2*p* core-level spectra at both temperatures. The experimental PED patterns of both the two surface components show good agreements with the simulated PED patterns obtained by considering the IET model. Further, the experimental PED patterns obtained at 10 and 300 K resemble each other closely. These results indicate that the local atomic structure of the Ag/Si(111)-( $\sqrt{3} \times \sqrt{3}$ ) surface follows the IET model at the two temperatures, and therefore that the transition reported in the literature originates from a thermally induced fluctuation of the IET structure at room temperature.

The PED measurements were performed at the beamline BL-1C at the Photon Factory of the High Energy Accelerator Research Organization, Tsukuba, Japan. Photoemission spectra were obtained using an angle-resolved photoelectron spectrometer with an acceptance angle of  $\pm 1^\circ$ . The total experimental energy resolution was  $\sim 120$  meV at  $h\nu = 140$  eV. An *n*-type (Sb-doped) Si(111) sample was cleaned by direct resistive heating up to 1500 K. After the annealing, a sharp ( $7 \times 7$ ) low-energy electron diffraction (LEED) pattern was observed, and neither the valence-band spectra nor the Si 2*p* core-level spectra showed any indication of contamination. The Ag/Si(111)-( $\sqrt{3} \times \sqrt{3}$ ) surface was prepared by depositing 1.2 ML of Ag onto a clean Si(111)-( $7 \times 7$ ) surface at a substrate temperature of  $\sim 800$  K, followed by further annealing at 870 K like the procedure described in Ref. 3. The quality of the Ag/Si(111)-( $\sqrt{3} \times \sqrt{3}$ ) surface was checked by the observation of a sharp ( $\sqrt{3} \times \sqrt{3}$ ) LEED pattern (Fig. 2), the observation of sharp surface states in the valence-band spectra, and the shape of the Si 2*p* core-level spectra. The base pressure was below  $1 \times 10^{-10}$  Torr during the measurements, and below  $3 \times 10^{-10}$  Torr during the Ag evaporation.

Figure 3 shows the Si 2*p* core-level spectrum obtained in the normal emission with a photon energy ( $h\nu$ ) of 140 eV after cooling the sample shown in Fig. 2 to 10 K. The incident angle of the *p*-polarized light was  $54^\circ$ . The open circles are the experimental data, and the solid line overlapping the open circles is the fitting curve obtained by a standard least-squares-fitting method using spin-orbit-split Voigt functions. We used 608 meV for the spin-orbit splitting, an 80 meV full width at half-maximum (FWHM) for the Lorentzian contribution, and a singularity index of 0.08 for all components in the fitting procedure. The Gaussian width was allowed to vary for the different components [the Gaussian widths of the B component is 180 meV (FWHM), and those of the S1 and S2 components are 195 and 210 meV (FWHM)]. A polynomial background was subtracted before the decomposition of the spectrum, and each component is indicated by differ-

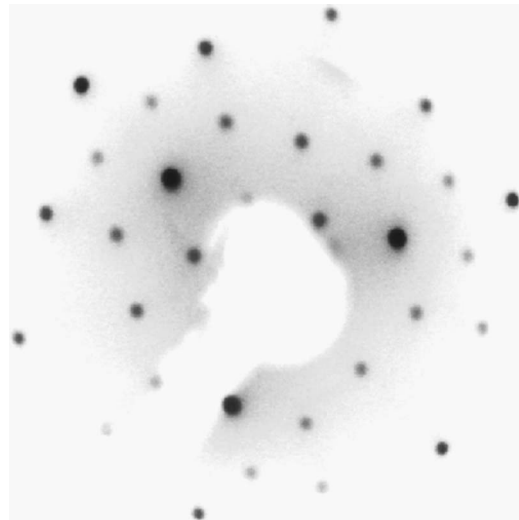


FIG. 2. LEED pattern of the Ag/Si(111)-( $\sqrt{3} \times \sqrt{3}$ ) surface obtained at 300 K with a primary electron energy of 160 eV.

ent hatching. The residual between the experimental data and fitting result is shown by a solid line at the bottom of the spectrum.

As displayed in Fig. 3, the fitting shows three major components of which one corresponds to the bulk Si atoms (B) and the other two (S1 and S2) to Si atoms of the reconstructed surface layers. The kinetic energies of the S1 and S2 components are shifted by  $-0.32$  and  $-0.13$  eV with respect

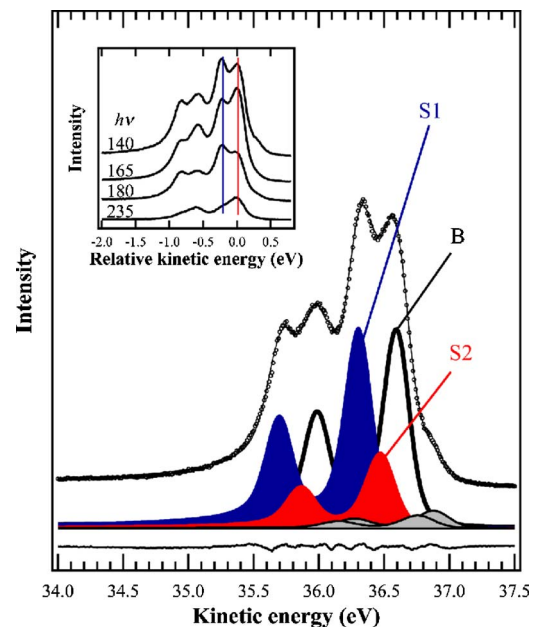


FIG. 3. (Color online) Si 2*p* core-level spectrum obtained after cooling the sample shown in Fig. 2 to 10 K. The photon energy and incident angle of the *p*-polarized light were 140 eV and  $54^\circ$ . The open circles are the experimental data, and the solid line overlapping the open circles is the fitting curve. Each component is indicated by different hatching. The residual between the experimental data and fitting result is shown by a solid line at the bottom of the spectrum. The inset shows the Si 2*p* core-level spectra obtained with different photon energies.

to the bulk component. These energies agree well with the energy shifts reported in the previous Si  $2p$  core-level studies,<sup>3,6</sup> and the intensity ratio of the three major components agrees well with the ratio obtained when using the same photon energy.<sup>6</sup> The good agreements in both the energy and the intensity support the validity of our fitting method. Further, since one more major component, whose kinetic energy is shifted by  $-0.45$  eV with respect to the bulk component, is needed in the case of a Ag/Si(111)-( $\sqrt{3} \times \sqrt{3}$ ) surface with low quality,<sup>6</sup> the result shown in Fig. 3 suggests that the quality of the sample used in the present study is as high as the samples used in the literature. Regarding the two small components observed at the higher kinetic side of the bulk component, their origins might be intrinsic defectlike domain boundaries as suggested in Ref. 3.

The inset of Fig. 3 displays the Si  $2p$  core-level spectra obtained with different photon energies. All the spectra are normalized by using the photon flux. As shown in this inset, the intensity ratio of the two peaks indicated by thin solid lines varies depending on the photon energy. Since this photon energy-dependent intensity variation results from a diffraction effect that originates from the difference in kinetic energy of photoelectrons, we have performed a photoelectron diffraction measurement in the so-called “energy scan mode” by measuring the interference patterns (or spectra) as a function of the kinetic energy of the emitted photoelectrons in the normal direction. The Si  $2p$  core-level spectra of the Ag/Si(111)-( $\sqrt{3} \times \sqrt{3}$ ) surface, which were measured every 5 eV from  $h\nu=135$  to 265 eV, have been fitted using spin-orbit split Voigt functions as well as the fitting shown in Fig. 3. In the fitting procedure, the Gaussian width was allowed to change since the total experimental energy resolution varies depending on the photon energy, but the Lorentzian width, the spin-orbit splitting, and the relative kinetic energies of the components were fixed. The filled circles in Fig. 4 are the photoelectron kinetic energy-dependent PED patterns of the S1 and S2 components obtained experimentally at 10 K, and the open circles are the PED patterns obtained experimentally at 300 K. As shown in Fig. 4, the PED patterns of each component are quite similar at the two temperatures. That is, the intensity of the S1 component first decreases as the kinetic energy increases, shows a dip at a kinetic energy of approximately 40 eV, increases until a kinetic energy of approximately 70 eV and shows a peak, and then decreases while showing three small structures at kinetic energies of approximately 85, 105, and 125 eV at both 10 and 300 K. Regarding the S2 component, it shows three structures at kinetic energies of approximately 65, 85, and 115 eV at the two temperatures.

In order to discuss the PED patterns in more detail, we compare the PED patterns obtained experimentally with the patterns obtained using multiple-scattering simulations. The simulations were performed using the multiple-scattering calculation of diffraction (MSCD) package developed by Chen and Van Hove.<sup>18</sup> The angle between the electric field vector of light and the sample, and the emission angle of photoelectrons used in the simulations, were the same as those used in the experiments. An IET model cluster and a HCT model cluster with radii of approximately 17 Å were used for simulations. Each cluster, which includes over 100

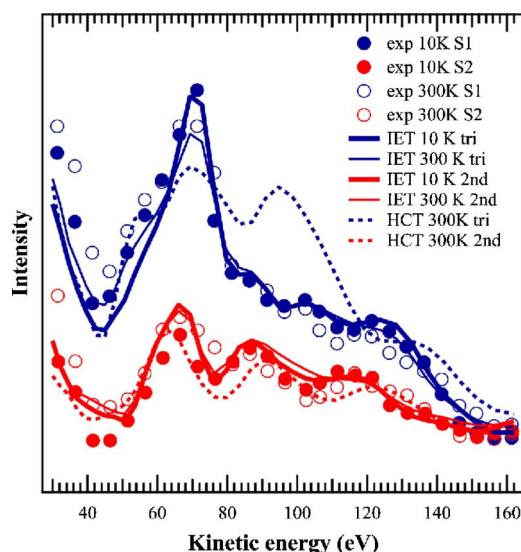


FIG. 4. (Color online) Photoelectron kinetic energy-dependent PED patterns of the two Si  $2p$  surface components of the Ag/Si(111)-( $\sqrt{3} \times \sqrt{3}$ ) surface. Filled circles and open circles are the experimental data obtained at 10 and 300 K, respectively. Thick and thin solid lines are the results of the multiple-scattering simulations for the IET model at 10 and 300 K, respectively, and the dashed lines are the result for the HCT model at 300 K.

atoms, was large enough to obtain a converged pattern, and the use of a larger cluster radius hardly affected the simulated PED pattern. The parameters described in Ref. 15 have been used to determine the positions of Si and Ag atoms of the clusters. The thick solid lines shown in Fig. 4 are the results of the multiple-scattering simulations for the IET model at 10 K, the thin solid lines are the simulated PED patterns for the IET model at 300 K, and the dashed lines are the results for the HCT model at 300 K. The simulated PED patterns described as “tri” are obtained by adding the PED patterns that result by considering the Si trimer atoms as emitters, i.e., the sum of the PED patterns that originate from the Si atoms numbered 4–9 in Fig. 1 for the IET model and those numbered 1–3 for the HCT model. The simulated patterns described as “2nd” are obtained by adding the patterns that originate from the second-layer Si atoms (the three Si atoms situated below the Si trimer atoms).

As shown in Fig. 4, the simulated “tri” patterns for the IET model are similar at 10 and 300 K, while the simulated “tri” pattern for the HCT model is different. The peak at approximately 70 eV and the three small structures at higher kinetic energies observed in the experimental PED pattern of the S1 component are well reproduced by the multiple-scattering simulations for the IET model. The simulations for the IET model also reproduce well the three structures of the S2 component. In contrast to the simulations for the IET model, the simulated PED patterns for the HCT model do not agree well with the PED patterns obtained experimentally. That is, although the simulated “2nd” pattern for the HCT model shows an agreement with the experimental result, the simulated “tri” pattern, which shows a huge peak at a kinetic energy of approximately 95 eV, is completely different. (We have also performed the fitting using the parameters reported

in Ref. 11, but these parameters did not give a better reproduction.) Taking the quite similar PED patterns obtained experimentally at 10 and 300 K and the simulated PED patterns into account, we conclude that the atomic structure of the Ag/Si(111)-( $\sqrt{3} \times \sqrt{3}$ ) surface follows the IET model at both temperatures, and therefore that the origin of the transition reported in the literature is an order-disorder transition. That is, the ground-state IET structure that is frozen at low temperature fluctuates at room temperature. Further, the good agreements between the experimental PED patterns and the simulated patterns support the assignments of the Si 2*p* surface components reported in the literature, i.e., the origin of the S1 component is the Si trimer atoms and the origin of the S2 component is the Si atoms of the second layer.

In conclusion, we have investigated the local atomic structure of the Ag-induced Si(111)-( $\sqrt{3} \times \sqrt{3}$ ) surface at 10 and 300 K using PED. In the Si 2*p* core-level spectra, two major surface components were observed at both temperatures. The intensities of the two surface components varied by changing the photon energy as a consequence of diffraction effects that originates from the difference in kinetic energy of photoelectron. The experimental PED patterns of the two surface components, which were obtained in the so-

called “energy scan mode” by analyzing the Si 2*p* core-level spectra measured every 5 eV from  $h\nu=135$  to 265 eV, resemble each other closely at the two temperatures. Further, both of the two surface components show good agreements with the simulated PED patterns obtained by considering the IET model. Taking these results into account, we conclude that the local atomic structure of the Ag/Si(111)-( $\sqrt{3} \times \sqrt{3}$ ) surface is the same IET structure at the two temperatures, and thus that the origin of the transition reported in the literature is an order-disorder transition. That is, the ground-state structure of this surface is IET, and the STM images observed at room temperature in the former studies result from the thermal fluctuation between the two IET structures that leads to an observation of the time-averaged structure. Moreover, the good agreements between the experimental and simulated PED patterns support the assignments of the Si 2*p* surface components reported in the literature.

#### ACKNOWLEDGMENTS

Experimental support from S. Toyoda, and suggestions on the analysis from M. Shimomura, T. Abukawa, and S. Kono, are gratefully acknowledged.

\*Electronic address: kazuyuki\_sakamoto@faculty.chiba-u.jp

<sup>1</sup>See, for example, J. M. Carpinelli, H. H. Weitering, E. W. Plummer, and R. Stumpf, *Nature* (London) **381**, 398 (1996); R. I. G. Uhrberg and T. Balasubramanian, *Phys. Rev. Lett.* **81**, 2108 (1998) for two-dimensional systems.

<sup>2</sup>See, for example, P. Segovia, D. Purdie, M. Hengsberger, and Y. Baer, *Nature* (London) **402**, 504 (1999); H. W. Yeom, S. Takeda, E. Rotenberg, I. Matsuda, K. Horikoshi, J. Schaefer, C. M. Lee, S. D. Kevan, T. Ohta, T. Nagao, and S. Hasegawa, *Phys. Rev. Lett.* **82**, 4898 (1999); K. Sakamoto, H. Ashima, H. M. Zhang, and R. I. G. Uhrberg, *Phys. Rev. B* **65**, 045305 (2002) for one-dimensional systems.

<sup>3</sup>R. I. G. Uhrberg, H. M. Zhang, T. Balasubramanian, E. Landemark, and H. W. Yeom, *Phys. Rev. B* **65**, 081305(R) (2002).

<sup>4</sup>H. M. Zhang, K. Sakamoto, and R. I. G. Uhrberg, *Phys. Rev. B* **64**, 245421 (2001).

<sup>5</sup>C. Liu, S. Yamazaki, R. Hobara, I. Matsuda, and S. Hasegawa, *Phys. Rev. B* **71**, 041310(R) (2005).

<sup>6</sup>H. M. Zhang, K. Sakamoto, and R. I. G. Uhrberg, *Phys. Rev. B* **70**, 245301 (2004).

<sup>7</sup>Y. G. Ding, C. T. Chan, and K. M. Ho, *Phys. Rev. Lett.* **67**, 1454 (1991); **69**, 2452 (1992).

<sup>8</sup>S. Watanabe, M. Aono, and M. Tsukada, *Phys. Rev. B* **44**, 8330

(1991).

<sup>9</sup>M. Katayama, R. S. Williams, M. Kato, E. Nomura, and M. Aono, *Phys. Rev. Lett.* **66**, 2762 (1991).

<sup>10</sup>T. Takahashi and S. Nakatani, *Surf. Sci.* **282**, 18 (1993).

<sup>11</sup>H. Aizawa, M. Tsukada, N. Sato, and S. Hasegawa, *Surf. Sci.* **429**, L509 (1999).

<sup>12</sup>N. Sato, T. Nagao, and S. Hasegawa, *Surf. Sci.* **442**, 65 (1999).

<sup>13</sup>I. Matsuda, H. Morikawa, C. Liu, S. Ohuchi, C. Hasegawa, T. Okuda, T. Kinoshita, C. Ottaviani, A. Cricenti, M. D'angelo, P. Soukiassian, and G. Le Lay, *Phys. Rev. B* **68**, 085407 (2003).

<sup>14</sup>Y. Kukaya, A. Kawasuso, K. Hayashi, and A. Ichimiya, *Appl. Surf. Sci.* **244**, 166 (2005).

<sup>15</sup>H. Tajiri, K. Sumitani, S. Nakatani, A. Nojima, T. Takahashi, K. Akimoto, H. Sugiyama, X. Zhang, and H. Kawata, *Phys. Rev. B* **68**, 035330 (2003).

<sup>16</sup>H. Nakahara, T. Suzuki, and A. Ichimiya, *Appl. Surf. Sci.* **234**, 292 (2004).

<sup>17</sup>L. Chen, H. J. Xiang, B. Li, A. Zhao, X. Xiao, J. Yang, J. G. Hou, and Q. Zhu, *Phys. Rev. B* **70**, 245431 (2004).

<sup>18</sup>Y. Chen, F. J. Garcia de Abajo, A. Chasse, R. X. Ynzunza, A. P. Kaduwela, M. A. Van Hove, and C. S. Fadley, *Phys. Rev. B* **58**, 13121 (1998).